PADF RF Localization Criteria for Multi-Model Scattering Environments

Miguel Gates [a], Christopher Barber [a], Rastko Selmic [a]
Huthaifa Al_Issa [b], Raul Ordonez [b], Atindra Mitra [c]
[a]Department of Electrical Engineering, Louisiana Tech University, Ruston, LA 71272
[b]Department of Electrical and Computer Engineering, University of Dayton, Dayton, OH 45469
[c]Air Force Research Laboratory, Wright-Patterson AFB, Dayton, OH 45433

ABSTRACT

This paper provides a summary of recent results on a novel multi-platform RF emitter localization technique denoted as Position-Adaptive RF Direction Finding (PADF). This basic PADF formulation is based on the investigation of iterative path-loss based (i.e. path loss exponent) metrics estimates that are measured across multiple platforms in order to robotically/intelligently adapt (i.e. self-adjust) the location of each distributed/cooperative platform. Recent results at the AFRL indicate that this position-adaptive approach shows potential for accurate emitter localization in challenging embedded multipath environments (i.e., urban environments). As part of a general introductory discussion on PADF techniques, this paper provides a summary of our recent results on PADF and includes a discussion on the underlying and enabling concepts that provide potential enhancements in RF localization accuracy in challenging environments. Also, an outline of recent results that incorporate sample approaches to real-time multi-platform data pruning is included as part of a discussion on potential approaches to refining a basic PADF technique in order to integrate and perform distributed self-sensitivity and self-consistency analysis as part of a PADF technique with distributed robotic/intelligent features. The focus of this paper is on the experimental performance analysis of hardware-simulated PADF environments that generate multiple simultaneous mode-adaptive scattering trends. We cite approaches to addressing PADF localization performance challenges in these multi-modal complex laboratory simulated environments via providing analysis of our multimodal experiment design together with analysis of the resulting hardware-simulated PADF data.

Keywords: Position-Adaptive Direction Finding, Micro Aerial Vehicles, Cooperative Control, RF Localization, Wireless Sensor Networks

1. INTRODUCTION

The concept of Position Adaptive Direction Finding (PADF) was introduced in [10]. PADF is based on the formulation and investigation of path-loss based metrics that are measured and estimated across multiple platforms in order to intelligently position-adapt the location of each platform. In other words, a sensor swarm adapts its position based on sensing values, dependent upon the medium, and converges towards leakage points in order to detect a hidden electromagnetic (EM) source. By using the relationship between Received Signal Strength (RSS) values and the associated distance between sender and receiver, the transmitter position can be approximated. We developed a set of experiments that reads sensor data, converts the data into approximate distance values based on approximated Path Loss Exponent (PLE) values, and estimates the position of the emitter using the Least Square Estimation (LSE) method. The algorithm is based on the LSE method described in detail in [5].

Mobile sensor networks and their application in sensing, localization, and control have gained significant interest with the development of sensor networks and modern control algorithms [2], [3], [4], [7], [13]. In accordance with previous works, cooperative control algorithms that maximize the probability of detection are given in [2], [7]. In addition, control and coordination for groups of autonomous vehicles performing distributed sensing was presented in [4]. With the development of micro-aerial vehicles (MAVs), cooperative control and sensing gained attention for applications such as military, weather forecast, chemical sensing, etc. A problem of cooperative path planning for a fleet of unmanned aerial vehicles in uncertain environments was presented in [3]. Similarly, a robust decentralized model predictive control for a

Report Documentation Page

Form Approved
OMB No. 0704-0188

1. REPORT DATE	2. REPORT TYPE	3. DATES COVERED
APR 2011		**00-00-2011 to 00-00-2011**

4. TITLE AND SUBTITLE	5a. CONTRACT NUMBER
PADF RF Localization Criteria for Multi-Model Scattering Environments	5b. GRANT NUMBER
	5c. PROGRAM ELEMENT NUMBER
6. AUTHOR(S)	5d. PROJECT NUMBER
	5e. TASK NUMBER
	5f. WORK UNIT NUMBER
7. PERFORMING ORGANIZATION NAME(S) AND ADDRESS(ES) **Air Force Research Laboratory,Wright-Patterson AFB,OH,45433**	8. PERFORMING ORGANIZATION REPORT NUMBER
9. SPONSORING/MONITORING AGENCY NAME(S) AND ADDRESS(ES)	10. SPONSOR/MONITOR'S ACRONYM(S)
	11. SPONSOR/MONITOR'S REPORT NUMBER(S)

12. DISTRIBUTION/AVAILABILITY STATEMENT
Approved for public release; distribution unlimited

13. SUPPLEMENTARY NOTES
Presented at SPIE Defense, Security Sensing Conference, Apr. 25 ? 29, 2011, Orlando Florida

14. ABSTRACT

This paper provides a summary of recent results on a novel multi-platform RF emitter localization technique denoted as Position-Adaptive RF Direction Finding (PADF). This basic PADF formulation is based on the investigation of iterative path-loss based (i.e. path loss exponent) metrics estimates that are measured across multiple platforms in order to robotically/intelligently adapt (i.e. self-adjust) the location of each distributed/cooperative platform. Recent results at the AFRL indicate that this position-adaptive approach shows potential for accurate emitter localization in challenging embedded multipath environments (i.e., urban environments). As part of a general introductory discussion on PADF techniques, this paper provides a summary of our recent results on PADF and includes a discussion on the underlying and enabling concepts that provide potential enhancements in RF localization accuracy in challenging environments. Also, an outline of recent results that incorporate sample approaches to real-time multi-platform data pruning is included as part of a discussion on potential approaches to refining a basic PADF technique in order to integrate and perform distributed self-sensitivity and self-consistency analysis as part of a PADF technique with distributed robotic/intelligent features. The focus of this paper is on the experimental performance analysis of hardware-simulated PADF environments that generate multiple simultaneous mode-adaptive scattering trends. We cite approaches to addressing PADF localization performance challenges in these multi-modal complex laboratory simulated environments via providing analysis of our multimodal experiment design together with analysis of the resulting hardware-simulated PADF data.

15. SUBJECT TERMS

16. SECURITY CLASSIFICATION OF:			17. LIMITATION OF ABSTRACT	18. NUMBER OF PAGES	19a. NAME OF RESPONSIBLE PERSON
a. REPORT **unclassified**	b. ABSTRACT **unclassified**	c. THIS PAGE **unclassified**	**Same as Report (SAR)**	**14**	

Standard Form 298 (Rev. 8-98)
Prescribed by ANSI Std Z39-18

team of aerial vehicles is given in [13] and for situations in urban terrain or urban battlefield in [15]. We present a set of experiments using static and mobile sensor networks to localize a non-cooperative sensor node based on measured RSS at surrounding sensor network. Related results are given in [11], [14]. We use on-line estimation of the PLE to model the distance based on measured RSS. A detailed analysis on PLE estimation and modeling is given in [8] which is then used in distance calculations based on RSS measurements.

This paper provides a discussion and a summary of the latest results on a novel sensor-node based approach to emitter localization that is PADF [1]. We demonstrate that this approach shows potential for accurate emitter localization in challenging embedded multipath environments (i.e. urban environments). Initial experimental test results (with ground-based distributed RF sensor nodes) conducted within the Louisiana Tech Micro-Aerial Vehicles and Sensor Networks (MAVSeN) laboratory indicate correlated trends between multi-platform RF-based control metrics formulated for this investigation and localization accuracy. These tests are conducted with an emitter inside a partially metal-sealed enclosure where varied hardware simulations are performed across several sets of discrete position-adaptive sensor node configurations/geometries. This paper is organized as follows: Section 2 introduces the concept of Position-Adaptive Direction-Finding (PADF) using cooperative Wireless Sensor Network (WSN) technologies; Section 3 explains the testing parameters and procedures of the experiment; Section 4 reveals the results from the aforementioned experiments; and Section 5 provides the summary and conclusion.

2. POSITION ADAPTIVE RF DIRECTION FINDING (PADF) CONCEPTS

Figure 1 illustrates two states of a notional PADF geometry using three UAV's that are integrated with sensor motes programmed to function as RF receivers. A theoretical signal analysis for this geometry is provided in [1] for purposes of formulating and illustrating this technique. The formulation and investigation of path-loss based (i.e. path loss exponent) metrics that are measured across multiple platforms are intrinsic to this technique. This formulation is described in detail in the following sections.

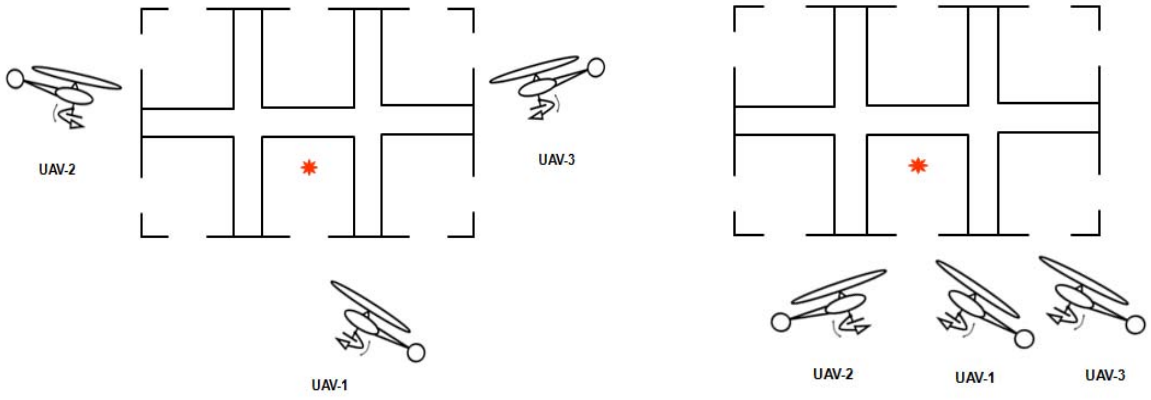

Figure 1: Initial PADF state transitioning into next stage after multi-platform adaptation [1]

2.1 PADF Formulation

Given two sensor nodes at locations $(x_i, y_i), (x_j, y_j)$, and an emitter in the *x*-*y* plane by vector $\mathbf{e} = (x, y)$, Euclidian distances between the emitter $\mathbf{e}$ and the sensors are given by

$$\begin{cases} r_i(\vec{x}) = \sqrt{(x - x_i)^2 + (y - y_i)^2} \\ r_j(\vec{x}) = \sqrt{(x - x_j)^2 + (y - y_j)^2} \end{cases} \quad (1)$$

Assume sensors provide enough information, using RRSI measurements, such that r_i and r_j are values that can be calculated based on RSSI data. The problem is to determine the location of the emitter $\mathbf{e} = (x, y)$, or equivalently, to solve two equations for two unknowns in (1). The solution to the system of equations is the intersections of the corresponding circles. However, three receiving nodes are required to precisely determine the position of the emitter. In case of N surrounding sensors, the problem is to determine the location of the emitter $\mathbf{e}$ or to solve the following system of equations

$$r_i = \sqrt{(x - x_i)^2 + (y - y_i)^2}, \quad i = 1,2,...,N. \tag{2}$$

Knowing that sensor measurements are noisy and that the system of equations (2) has larger number of equations than unknowns, we use LSE to determine the location estimate $(\hat{x}, \hat{y})$. The PLE depends on the medium of EM signal propagation and is not known a priori. Consider the model given in
Figure 2 consisting of a network of sensors S_i (i=1,2,3,4) and a non-cooperative emitter S_0. Distance between nodes i and j is denoted as d_{ij}. The signal strength received from node i at node j is denoted as P_{ij}.

Assumption 1. A symmetric wireless signal propagation model is considered, i.e., $P_{ij} = P_{ji}$ for $i, j \in \{0,1,2,3,4\}$.

Assumption 2. Location of sensor nodes S_i (i=1,2,3,4) is known. Location is an emitter S_i is unknown.

The received signal strength (RSS) model is given by

$$P_{ij}(dBm) = P_0(dBm) - 10 \cdot \alpha \cdot \log(d_{ij} / d_0) \tag{3}$$

where a is a Path Loss Exponent (PLE), $P_{ij}(dBm)$ is power received at node j from node i in dB milliwatts and $P_0(dBm)$ is a reference power received at some distance d_0. Note that the calibration method requires measurements of P_0 and d_0.

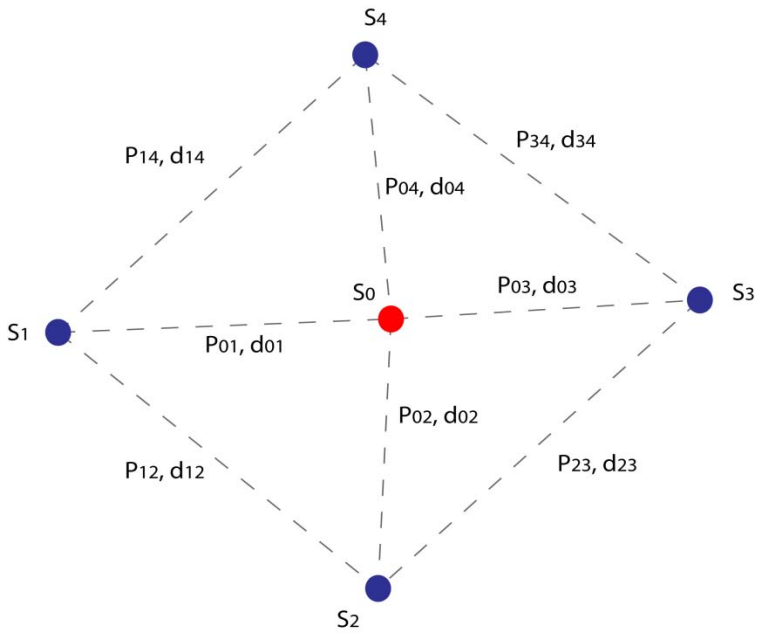

Figure 2: Model of a sensor network used to localize a non-cooperative emitter

2.2 Emitter Localization Estimation

The PLE estimation is given by the following optimization problem where it is required to find a minimum of the quadratic function $f(a)$

$$f(\alpha) = \sum_{i,j=1,2,3,4} \left(P_{ij}(dBm) - P_0(dBm) + 10 \cdot PLE \cdot \log(d_{ij}/d_0) \right)^2 . \quad (4)$$

The optimal value of the *PLE* is given by

$$\frac{\partial f(\alpha)}{\partial \alpha} = 2 \sum_{i,j=1,2,3,4} 10 \log(d_{ij}/d_0) \left(P_{ij}(dBm) - P_0(dBm) + 10 \cdot PLE \cdot \log(d_{ij}/d_0) \right) = 0 . \quad (5)$$

Therefore, the solution is given by

$$\alpha = \frac{\sum_{i,j=1,2,3,4} \log(d_{ij}/d_0) \left(P_0(dBm) - P_{ij}(dBm) \right)}{\sum_{i,j=1,2,3,4} \log(d_{ij}/d_0)} . \quad (6)$$

Such obtained value of *PLE* represents a maximum likelihood estimator value. Note also that calculation of PLE given by (6) requires prior calibration between sensors S_i (i=1,2,3,4). In case that there are more than found (4) nodes, the formula (6) still applies requiring just larger number of sensor nodes to be considered.

2.3 RSSI Model on IRIS Sensor Nodes

If distances r_i and r_j in (1) are not known, they can be calculated based on RSSI data. The RSSI model that is used is given by

$$RSSI = -10 \cdot \alpha \cdot \log(D) - K , \quad (7)$$

where a is the PLE, D is the distance between transmitter and receiver, and K is the conversion constant of RSSI to *dBm* (in this case -91). Therefore, the distance is given by

$$D = 10^{-\frac{RSSI + K}{10 \cdot \alpha}} . \quad (8)$$

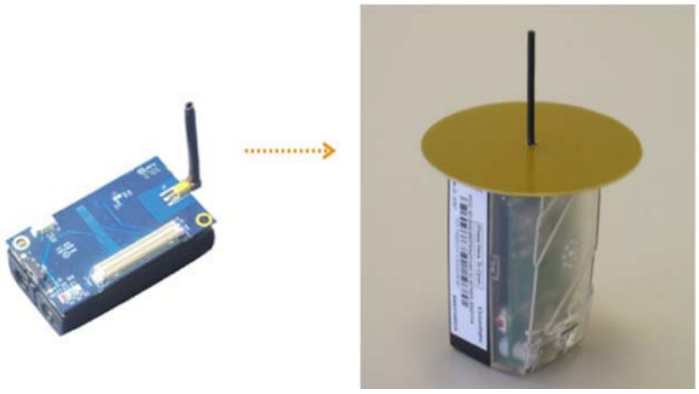

Figure 3: Modified IRIS sensor node for improved omnidirectional RSSI measurements.

2.4 MEMSIC IRIS nodes

The sensor nodes that were used for the experiments were the IRIS nodes. The IRIS 2.4 GHz mote by MEMSIC is a module used for enabling low-power, wireless sensor networks [9]. It has a 2.4 to 2.48 GHz globally compatible ISM band; a 250 kbps high data rate radio (outdoor line-of-sight tests yielded ranges as far as 500 meters between nodes without amplification); an IEEE 802.15.4 compliant RF transceiver; and a direct sequence spread spectrum radio (resistant to RF interference/provides inherent data security.) These nodes are the basis for the detection of the EM transmitter. We use four nodes in the development stage to test the functionality of PADF. Their primary function is not only to detect the EM source, but also transmit the RSSI values between neighboring nodes and the transmitter. These RSSI values will be instrumental in determining the position of the transmitter. As seen in
Figure 3, the antenna was customized by adding a ground plane to restrict interference of the EM signal by the node's internal circuitry. This modification allowed for relatively omni-directional RSSI measurements.

3. EXPERIMENTS AT MAVSEN LABORATORY

In order to further investigate PADF concepts in an indoor laboratory environment, we implemented a series of experiments at Louisiana Tech University's Micro-Aerial Vehicles and Sensor Networks (MAVSeN) laboratory. The MAVSeN lab was designed specifically for the purpose of research in small-scale aerial vehicle design, cooperative intelligent sensing, and control algorithms of such platforms for various applications. The laboratory has unique capabilities for experimenting with swarms of MAVs and sensor networks, in both layered and cooperative sensing concepts. The laboratory setup provides a high-speed and high-resolution motion capture system that emulates indoor GPS. The motion capture system has the ability to track markers ranging from 3-24mm. Any objects that can be outfitted with at least four markers, placed in distinct positions, are able to be tracked by the cameras.

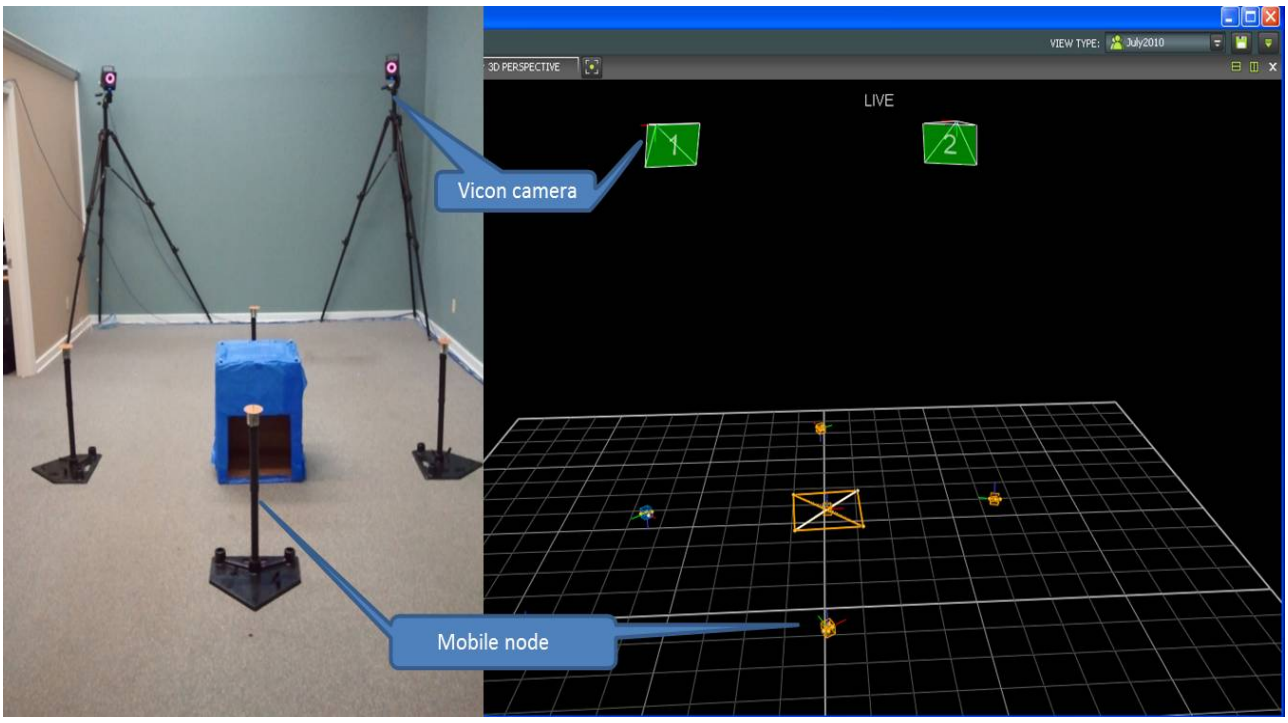

Figure 4: MAVSEN Lab Facility with RF emitter located inside partially open blue metal enclosure and four cooperative position-adaptive sensor stands configured for PADF hardware simulation experiments. Relationship between real world experiment versus Vicon Tracker software positioning station display is depicted

3.1 Collecting Data Autonomously

The Vicon system provides tracking of any object outfitted with specialized tracking markers, as an object inside the system's capture volume, thus providing an indoor "GPS-like" environment. This adds precision and accuracy to measuring the position of the IRIS nodes inside of the experimental space. Using the Tracker software that comes standard with the Vicon system [17], Figure 4 shows how a real-world experimental setup can be tracked via the software. In this scenario, each node is configured with at least four tracking markers in a distinctive and unique pattern—this allows each configured object to be tracked individually. The Vicon system is able to get the *x*, *y*, and *z* coordinate of each marker on the object. It sends this position to the Giganet switch, which acts like a hub for all the data being streamed in. This data is then sent to the server, where we have access to it. Because all the data is streamed in at once, we sort and parse the data for each of the five objects—one emitter and four IRIS nodes, respectively. The emitter is placed inside the blue box. The box is lined in foil that restricts EM propagation except at the opening, which is considered a leakage point. Such setup simulates an urban environment and tests the ability of the nodes to effectively track and localize a hidden emitter.

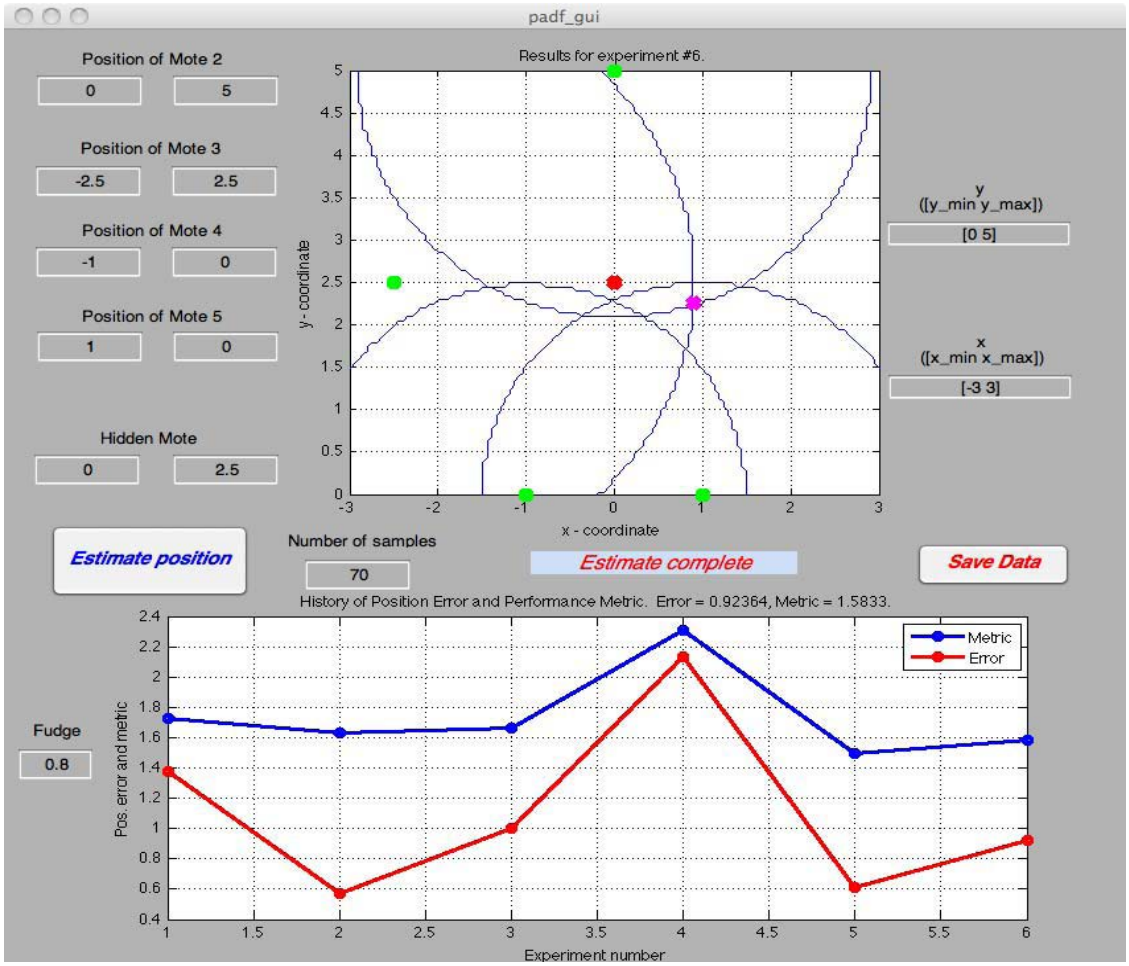

Figure 5: MATLAB GUI for PADF calculation [11]

3.2 Importing Data into MATLAB

We have developed a GUI using MATLAB that allows for easy implementation of the PADF concepts, as seen in Figure 5 [11]. The GUI takes the Cartesian coordinates (inside a Gaussian space) of known nodes, along with the hidden emitter, and gives a prediction or estimation as to where the hidden node could be. Each green dot represents one of the known nodes, or receivers. The red dot in the center represents the actual hidden emitter location. The pink dot represents the hidden emitter's estimated position. Based on the location of actual compared to estimated, we determine an absolute error, which shows the accuracy of the localization technique. For a proof of concept, we know the location of the hidden emitter. For a real-world exercise, this knowledge would not be privy. To overcome this dilemma, a metric was created that follows the trend of accuracy, thus giving us the ability to determine the location of the emitter by knowing which configurations will yield the best results. The GUI itself has two modes in which to input the position of the nodes: a manual configuration and an autonomous configuration. The manual mode allows a user to input the coordinates of the objects in their respective input boxes. The autonomous mode, however, gets the position data directly from the Vicon software in accordance to the positions of the tracked objects. This procedure is described in Figure 5. The Vicon system tracks the luminescent markers on each object and sends this data to the Vicon server. Because there are four markers per object, each object is composed of a 16-element array that has *x*, *y*, *z* coordinates as well as an occluded flag, that determines if the marker can be seen. The data stored on the Vicon server is then transferred to a separate station via a CAT-5 crossover cable. This station has the MATLAB with specialized GUI. The z-coordinate is disregarded, as well as the occluded, for the purpose of measurements necessary in the GUI calculations. The four *x* and *y* positions are used to calculate a centroid for the object's position. On the other side of the loop, the IRIS nodes themselves gather the RSS from emitter to receiver and forward that information to the base station wirelessly, which is then sent to the same MATLAB station via USB. The GUI merges the position data of the nodes as well as its corresponding RSSI measurements, and performs the LSE in order to estimate the location of the hidden emitter.

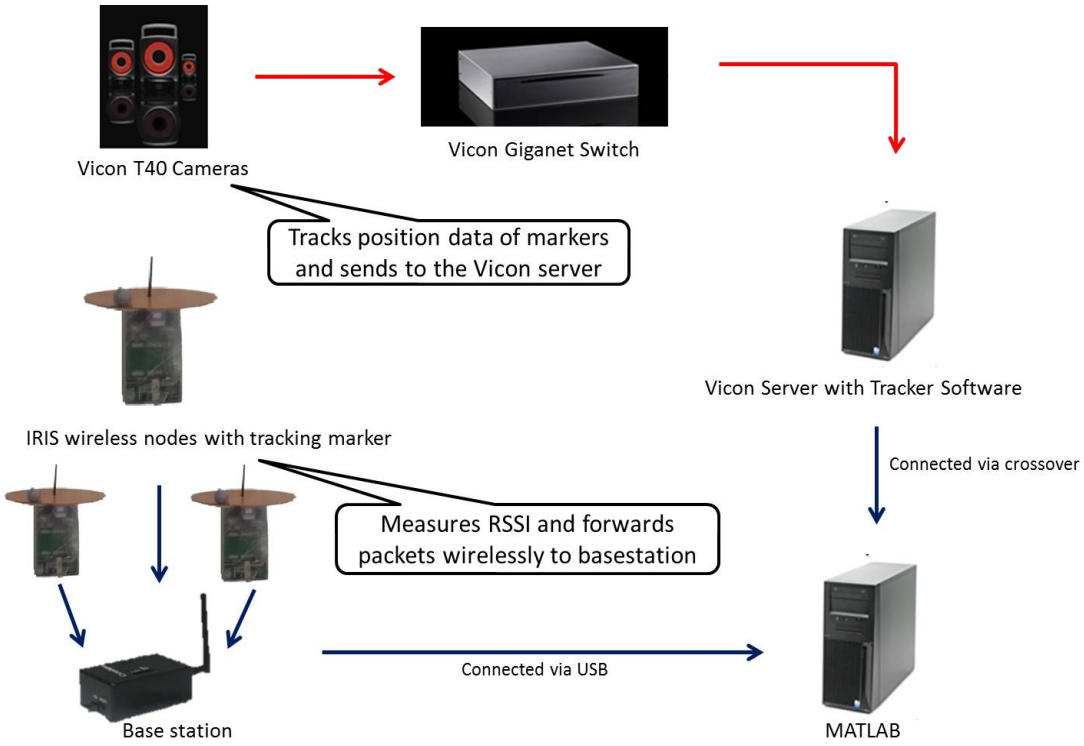

Figure 6: Position data flow from Vicon to MATLAB

3.3 Experimental Procedures

The latest experiment was developed with the purposes of investigating potential refinements in consistency, sensitivity, and robustness via the design and implementation of three stationary platforms and one continuously moving platform. A defined experiment configuration is shown in Figure 7, where the green dots represent the position of the static nodes; the red dot represents the actual position of the hidden emitter; and the series of blue dots represent the moving trajectory of the mobile node. The node moved in a "zig-zag" pattern towards the opening of the box, taking measurements at eight distinct waypoints in between. There were 512 RSSI samples taken at each waypoint, which will be instrumental in processing the results of the data, and determining the sensitivity of a specific configuration.

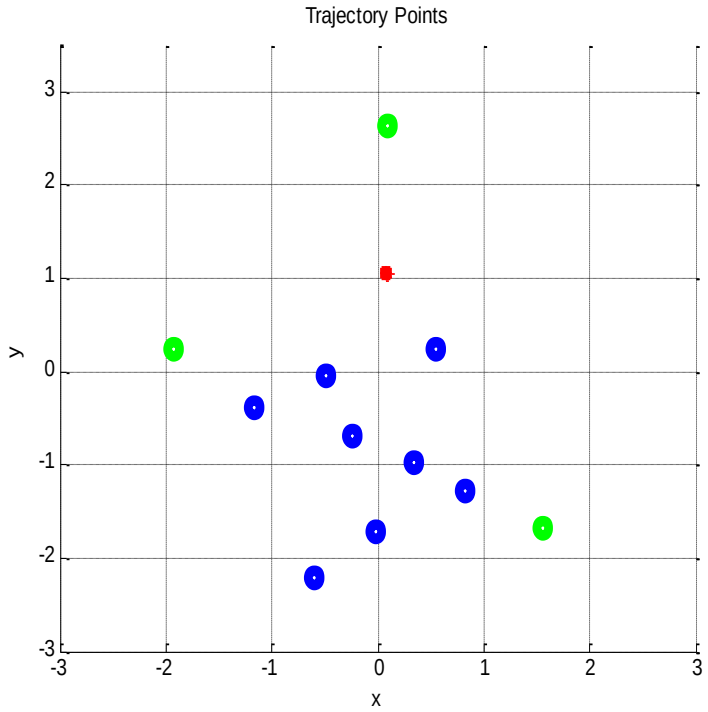

Figure 7: Trajectory of mobile node in sensitivity experiment

4. Results And Scope For Future Research

In this section, we provide a discussion and analysis results from a sample of set of recent position-adaptive direction finding (PADF) experiments. As outlined in the previous sections, the flavor of this investigation is towards the development of intelligent cooperative multiplatform position-adaptive (robotics) integrated sensor/platform development via the leveraging of very low-cost technologies. These adopted technologies such as readily accessible sensor motes with low-cost non-coherent RSSI measurement functionalities typically can enable the development of rudimentary direction-finding capabilities with somewhat degraded accuracy/performance characteristics in relation to techniques that can be developed via the design of more expensive coherent measurement systems. Therefore, our primary focus is to formulate and investigate intelligent multi-platform cooperative techniques that drastically trade-off hardware costs in favor of the development of new and sophisticated self-adaptive and onboard self-analysis techniques that evaluate RF scatterering trends in real-time. This type of approach shows potential for leading to the development of new generations of low-cost robotic-type platforms with ingrained capabilities to measure and position-adaptively respond to a given RF scattering environment for purposes of facilitating more accurate RF system performance via the employment of very low-cost hardware combined with new techniques such as cooperative self-pruning of RF data.

We initiate this discussion by considering a limited set of data collected at the AFRL MAV in early July 2010 [11]. The structure of these experiments are depicted in Figure 8 where we have three stationary sensor nodes and one moving sensor that position-adaptively traverses a 10-point zigzag trajectory. This moving sensor is the silver RC-vehicle shown towards the front of Figure 8 in the right-half of the figure. Figure 9 illustrates some desirable properties of potential PADF metrics developed for this investigation in the sense that the PLE (Cooperative Multiplatform Path Loss Estimate) RF-scattering-based multiplatform control metric computation (blue curve) displays the same general trends as the error metric (red curve). In addition, observation of distance estimate computations, D (green curve), from the moving sensor to the embedded emitter indicate that flat regions in D can be used for onboard robotic self-sensitivity/consistency analysis for purposes of electronically determining appropriate position-adaptive multi-platform coordinate sets within the platform trajectories/trajectory that can lead to low errors in RF emitter localization estimates. For example, in Figure 9, the first three point in D (green curve) comprise a flat region where minima in the localization error are strongly consistent with minima in the cooperative multi-platform PLE RF scattering-based control metric. Additional details pertaining to the development of this particular experimental multiplatform RF-scattering-based PLE metric are provided in [1] and [11].

Additional approaches to developing cooperative self-refining techniques for multiplatform PADF can be investigated via the consideration and integration of multi-model scattering analysis techniques such as cepstrum analysis [18] [19]. This basic approach is illustrated in Figure 10 where the left-half of the figure is an analytical model for a signal with two multipath delay components and the right-half of Figure 10 represents the corresponding multipath spectrum. One straightforward approach to robotic self-consistency/sensitivity analysis of RF multipath scattering can be considered via implementation of fft-based complex cepstrum computations:

$$ccep = ifft(\log(abs(fft(w.*s)))) \tag{9}$$

where log represents a vector complex logarithm operation, w represents a vector window function, and s is a signal vector measured at the moving sensor in Figure 8 that traverses a 10-point zigzag trajectory.

Since the complex cepstrum can be interpreted as representing the logarithmically-weighted components of the signal spectrum (i.e. right half of Figure 10), sharp peaks in the middle and upper "qfrequency" regions of the complex cepstrum (as a function of spatial trajectory coordinates) can represent sensitivities and consistencies in complex multi-modal scattering environments over small localized portions of a platform trajectory. Isolation of these types of localized regions can, in turn, provide information with respect to the consistency/sensitivity of potential multi-platform RF-scattering-based PLE-type metrics that are under consideration for the facilitation of robotic PADF self-localization convergence over a given region that is within a cooperative multi-platform trajectory space. For example, observation of the spatially distributed complex cepstrum in Figure 11 that is computed for the 10-point zigzag trajectory in Figure 8 in comparison to the corresponding PLE RF scattering-based multiplatform control metric and localization error curve in Figure 9 reveals some interesting inverse correlations. For example, points 2 and 6 in Figure 9 correspond to local maxima in localization error whereas observation of the complex cepstrum for points 2 and 7 in Figure 11 reveal distinct multipath signal delay component coupling patterns for this particular 10-point zigzag pattern (measured at the moving zigzag sensor.)

Similarly, a geometry for PADF data recently collected at the MAVSEN lab with a 8-point zigzag sensor-stand trajectory is depicted in Figures 12, 13, and 14. For this particular experiment, the discrete set of position-adaptive trajectory points yield good convergence to low values for the localization errors. However, comparison of the fifth point in Figure 13 for the RF-scattering-based PLE multi-platform control metric (blue curve) in relation to the localization error (red curve) yields a divergence between the local RF multiplatform control metric minima and localization error. This divergence effect may be due to direct coupling effects between the moving sensor and the sensor that is located behind the partially open metal enclosure and can be attributed to the relative height of the sensor stands in relation to the enclosure in terms of possible degradations in measuring and estimating basic scattering effects with our current experimental PLE control metric computation. Performance enhancements that accommodate for this type of effect will be investigated as part of a follow-up analysis. Approaches to follow-up investigation include formulating additional PLE control metric computations that account for direct coupling between sensors, incorporation additional levels of multiplatform position-adaptation onto our experiments, and additional low-cost hardware

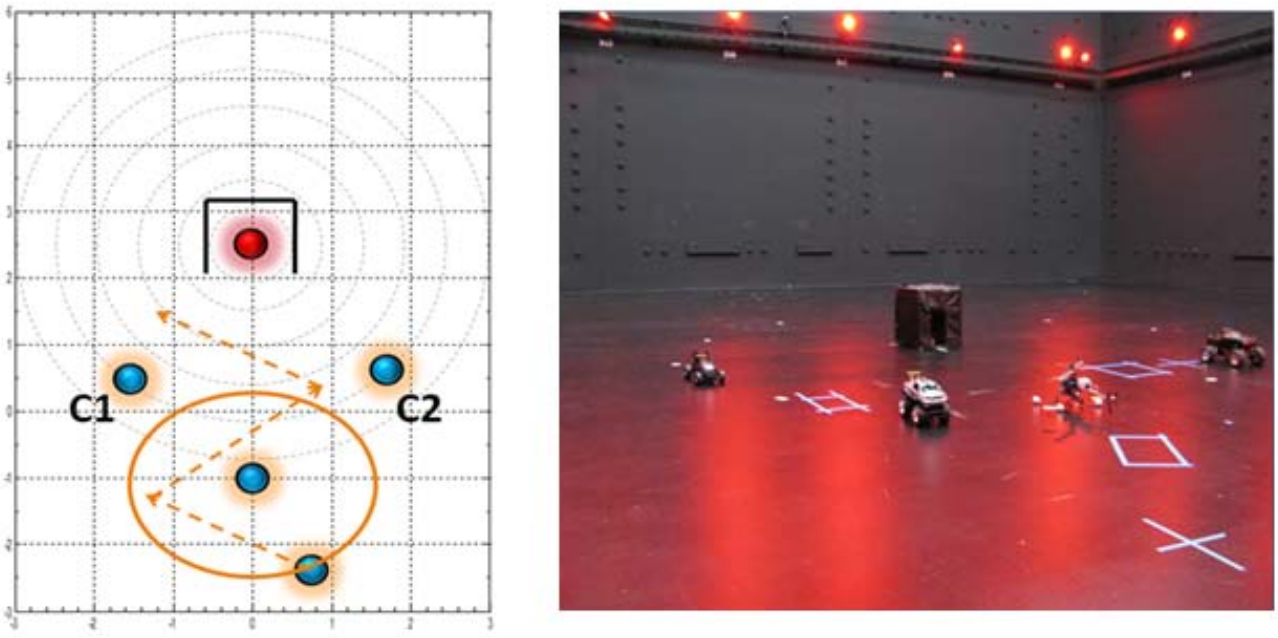

Figure 8: Experiment with zigzag trajectory conducted at AFRL MAV Lab Facility. Silver vehicle towards the front contains moving position-adaptive sensor with zigzag trajectory [11]

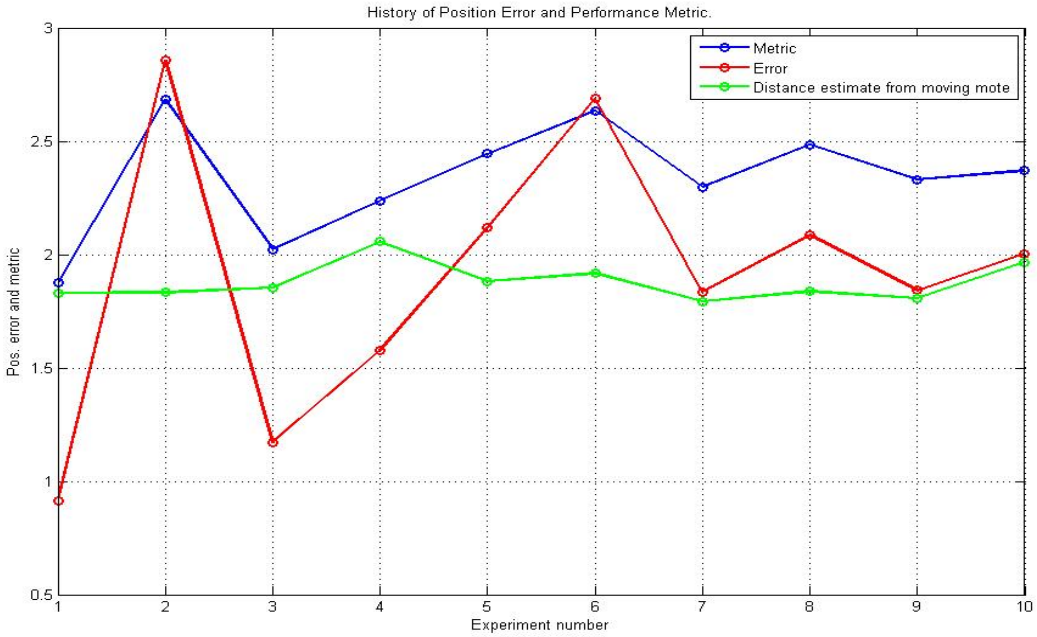

Figure 9: Analytical plots for 10-point zigzag trajectory experiment depicted in Figure 8 illustrating correlated trends between RF-scattering based cooperative multi-platform position-adaptive control metric (blue curve), error metric (red curve), and distance estimate from moving zigzag sensor to RF emitter [11]

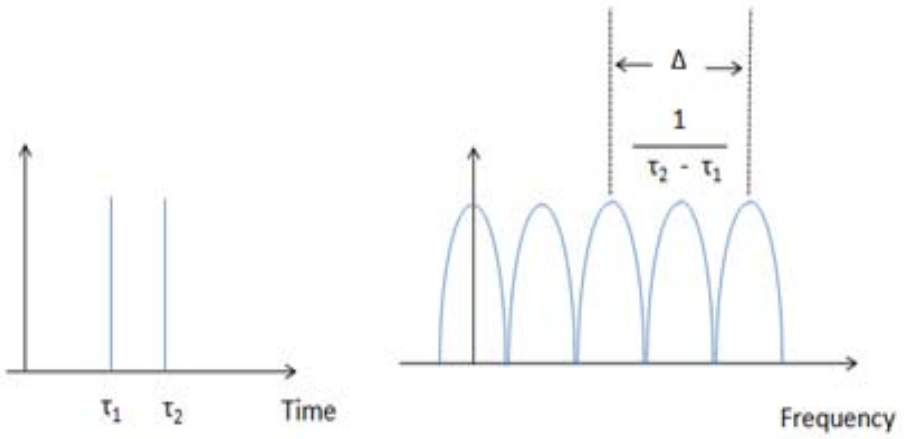

Figure 10: Analytical model for investigating the development of intelligent multipath echo trend computations within cooperative PADF RF-scattering-based multi-platform control loop [18]

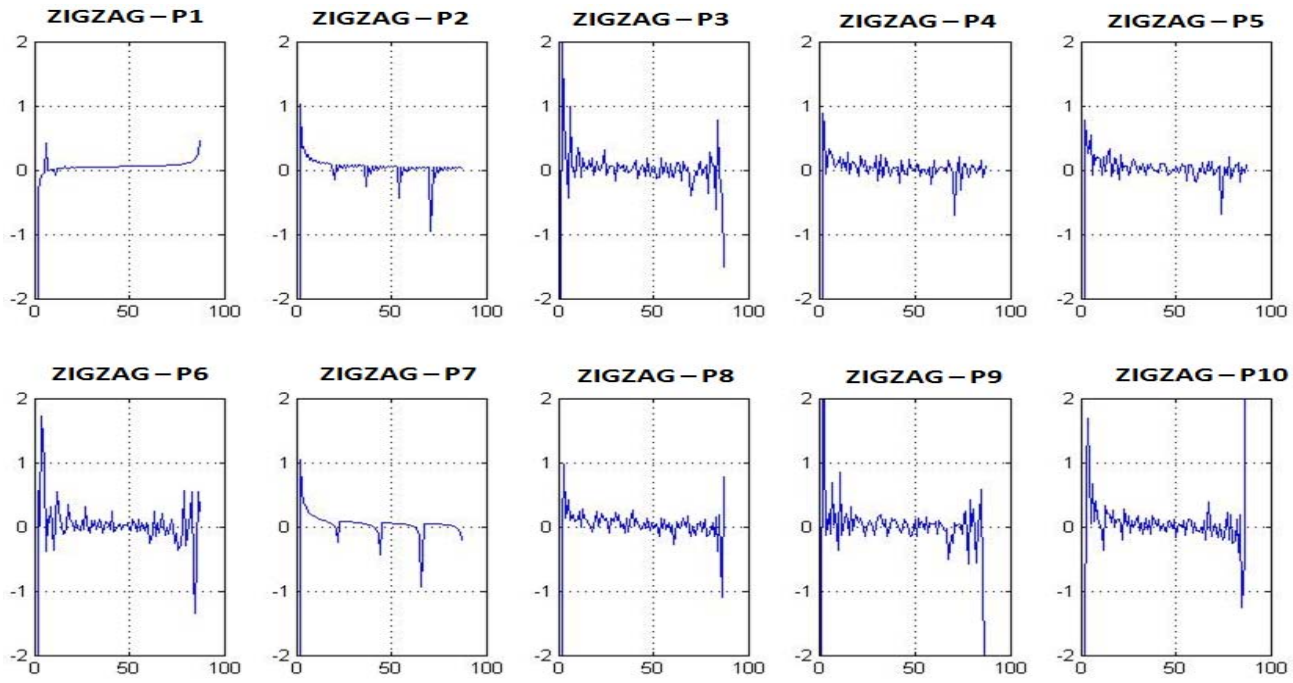

Figure 11: Complex cepstrum analysis of non-coherent (RSSI) multipath echo trends for 10-point zigzag experiment depicted in Figures 8 and 9

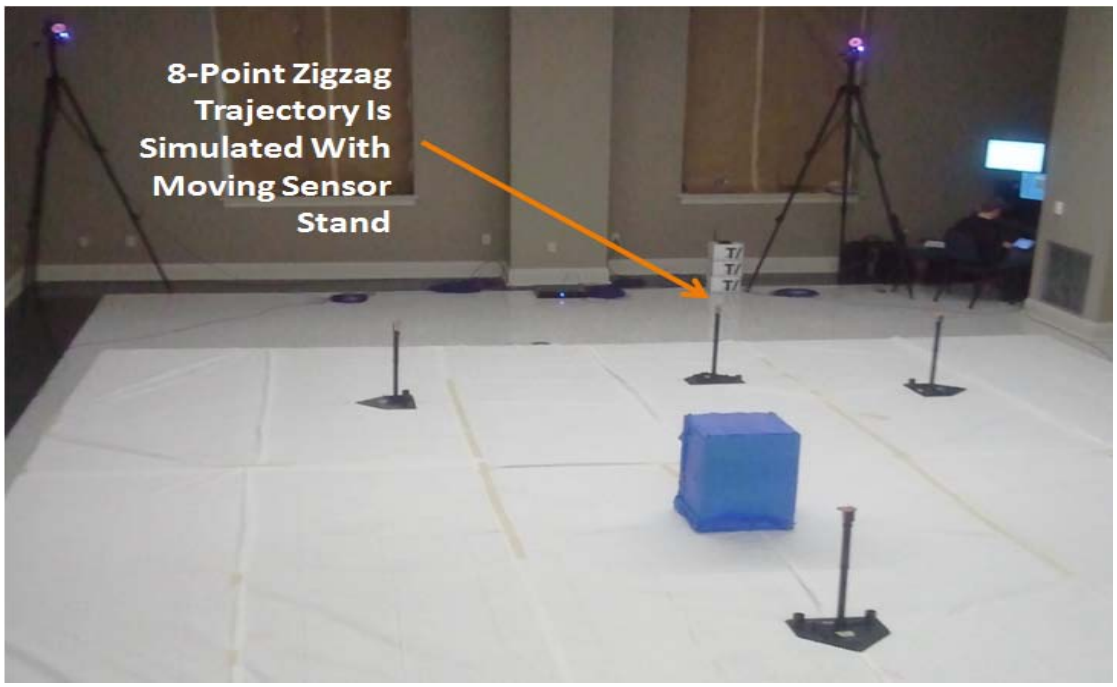

Figure 12: Experiment with simulated 8-point zigzag trajectory conducted at MAVSEB Lab Facility (RF emitter is located inside partially open blue metal enclosure)

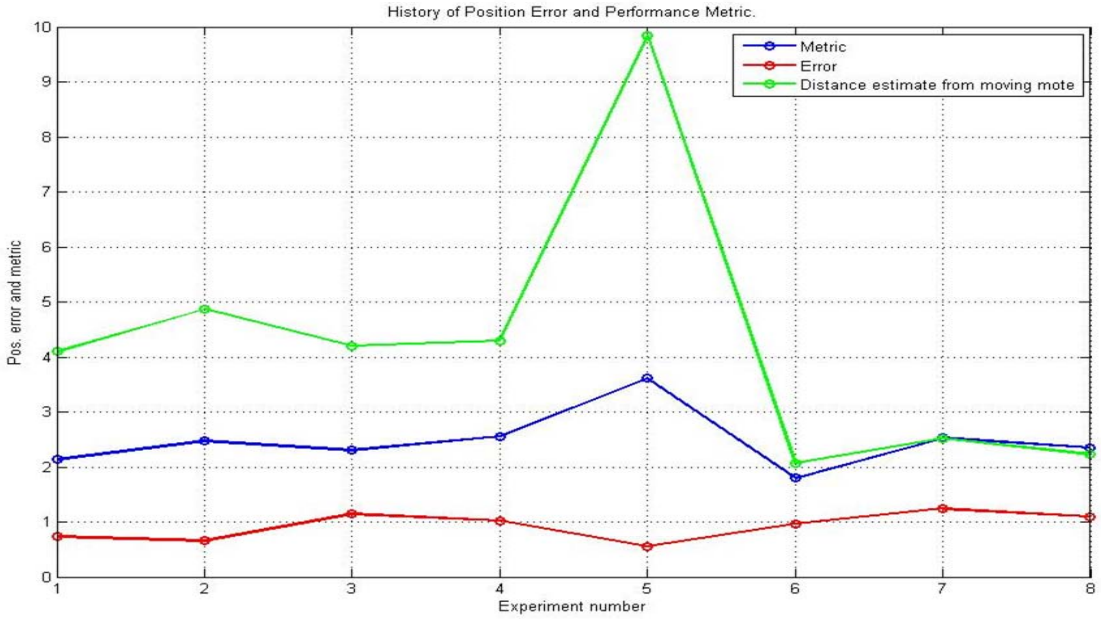

Figure 13: Analytical plots for 8-point zigzag trajectory experiment depicted in Figure 12 illustrating point-by-point measurements of RF-scattering based cooperative multi-platform position-adaptive control metric (blue curve), error metric (red curve), and distance estimate from moving zigzag sensor to RF emitter

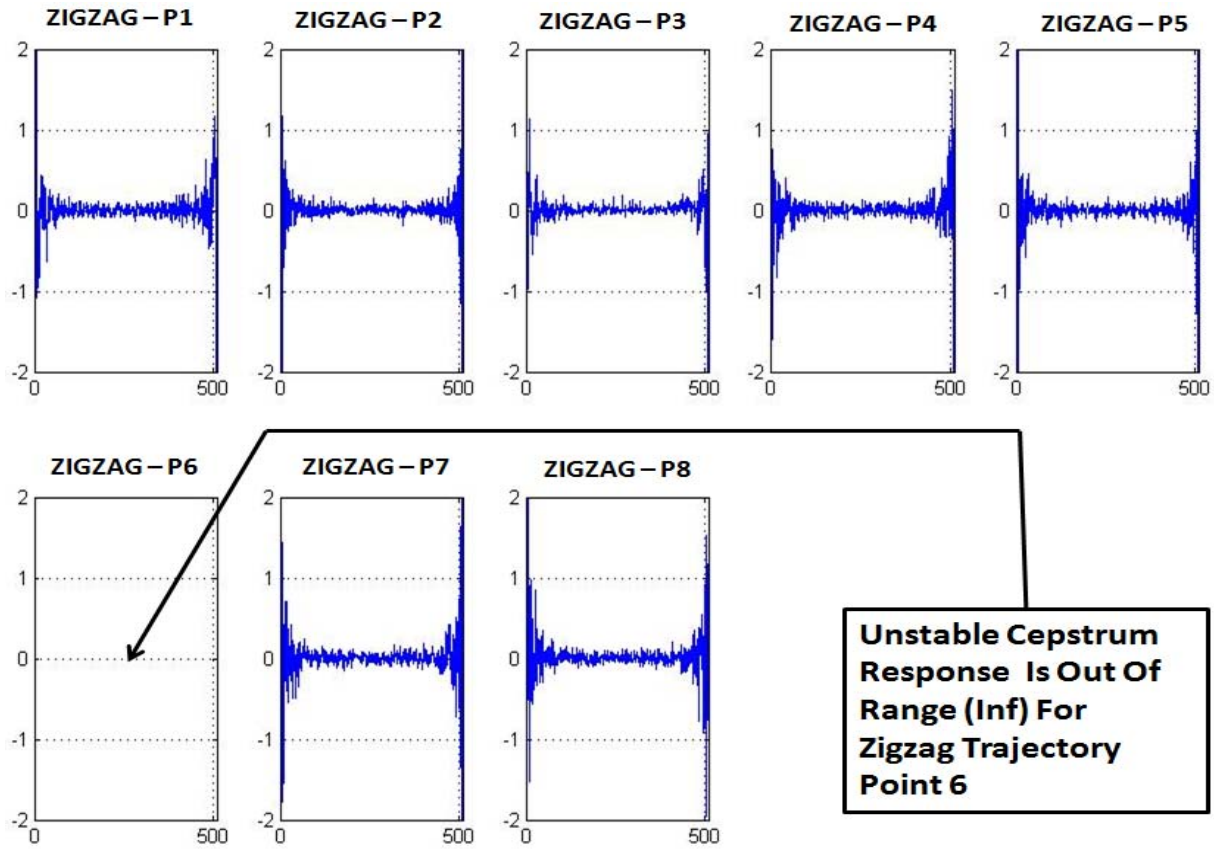

Figure 14: Complex cepstrum analysis of non-coherent (RSSI) multipath echo trends for 8-point zigzag experiment depicted in Figures 12 and 13

integrated aperture upgrades including platforms diversity/mobility in terms of incorporating platform robotic degrees-of-freedom in terms of platform aperture orientations.

One feature that can be associated with the present experimental approach can be observed the plots of Figure 13 as follows: Point number 5 in Figure 14, or the divergence point between the local PLE multiplatform control metric maxima and localization error, can be mitigated by observation of the corresponding non-flat region in the green curve for D, the distance estimate from the moving sensor. This approach always for the selection of another region of the curve for purposes of generating accurate localization estimates. In addition, comparison of Figures 13 and 14 yields divergence between the PLE-based control metric and localization error at point 5 in Figure 13 in comparison with cepstrum computational instabilities at point 6 in Figure 14. The remainder of the cepstrum curves in Figure 14 for the additional points in the 8-point ceptrum trajectory do not seem to indicate any distinct structure of cepstrum peaks and may indicate the lack of strong multi-modal signal time delay multipath echo components and seem to be consistent with the relatively low localization error levels in Figure 13.

These initial trends in RF-measurement-based PLE scattering metrics for multi-platform cooperative robotic control with a focus on radar and RF direction finding applications will be investigated in more detail both at an analytical and experimental level in follow-up investigations and respective correspondence. Also, additional interesting concepts for potential future research include the investigation of passive and active position-adaptive radar/RF systems concepts that incorporate multiple/distributed wireless/mobile-integrated EO and RF sensors for intelligent scattering-based position-adaptive multiplatform control via design and implementation with computational resources that incorporate a number of recent advances in mobile and distributed computing architectures [20] [21].

REFERENCES

[1] A. Mitra, et. al. “Sensor Agnostics for Networked MAV Applications,” Proceedings of the 2010 SPIE Defense, Security, and Sensing Symposium, Evolutionary and Bio-Inspired Computation: Theory and Applications IV, Vol. 7704, 15 April 2010

[2] Cassandras, C. G., and Li, W., “Sensor networks and cooperative control”. European Journal of Control, 11:436-463, June 2005.

[3] Chandler, P. R., Patcher, M., and Rasmussen, S., “UAV cooperative control”. In Proceedings of the American Control Conference, Arlington, VA, June 2001.

[4] Cortes, J., Martinez, S., Karatas, T., and Bullo, F., “Coverage control for mobile sensing networks”. IEEE Transactions on Robotics and Automation, 20(2):243-255, 2004.

[5] Feldmann, S., Kyamakya, K., Zapater, A., and Lue, Z., “An Indoor Bluetooth-based positioning system: concept, implementation, and experimental evaluation.” Technical report, University of Hannover, (2003).

[6] Gates, M., Barber, C., Selmic, R., Duncan, C., and Kanno, J., “Micro-Aerial Vehicle and Sensor Networks Laboratory Development and Applications”, Proc. of 3rd Cyberspace Research Workshop, Shreveport, LA, November 2010.

[7] Li, W. and Cassandras, C. G., “Distributed cooperative coverage control of sensor networks”. In Proceedings of 44th IEEE Conference on Decision and Control, Seville, Spain, December 2005.

[8] Mao, G., Anderson, B., and Fidan, B., “Path loss exponent estimation for wireless sensor network localization,” Computer Networks, vol. 51, no. 10, pp. 2467-2483, July 2007.

[9] MEMSIC. Wireless sensor networks. http://www.memsic.com/products/wireless-sensor-networks.html.

[10] Mitra, A. K., “Position-Adaptive UAV Radar for Urban Environments,” Proc. of the IEEE International Radar Conference, Adelaide, Australia, 2003.

[11] Ordonez, R., Gates, M., Moma, K., Mitra, A., Selmic, R., Detweiler, P., Cox, C., Parker, G., Goff, Z., “RF emitter localization with position adaptive MAV platforms,” Proc. 2010 IEEE NAECON, Dayton, July 2010.

[12] Quanser. Unmanned systems. http://www.quanser.com/english/html/UVS_Lab/fs_overview.htm.

[13] Richards, A. and How, J. “Decentralized model predictive control of cooperating UAVs”. In Proceedings of 43rd IEEE Conference on Decision and Control, Atlantis, Paradise Island, Bahamas, December 2004.

[14] Sichitiu, M. L., Ramadurai, V., “Localization of wireless sensor networks with a mobile beacon,” 2004 IEEE International Conference on Mobile Ad-hoc and Sensor Systems, Oct. 2004.

[15] Singh, L. and Fuller, J. “Trajectory generation for a UAV in urban terrain, using nonlinear MPC”. In Proceedings of the American Control Conference, Adelaide, Australia, 2003.

[16] TinyOS. Retrieved from www.tinyos.net, 2010.

[17] Vicon. Vicon t40 cameras. http://vicon.com/products/t40.html.

[18] Atindra K. Mitra “Multitone Radar Design Using Software Radio Components,” Radar Sensor Technology XIII, SPIE Defense and Security Symposium, Orlando, Florida, April 2009

[19] Atindra K. Mitra “Position-Adaptive Multiplatform Control for RF Measurement Applications,” White Paper Proposal Submitted for 2011 AFRL Sensors Directorate Entrepreneurial Research Program, November 2010

[20] Atindra K. Mitra, “Position-Adaptive Sensors,” *2008-2011 Air Force Summer Faculty Fellowship Program Topic*

[21] April Johnson, Cara Rupp, Brad Wolf, Lang Hong, Atindra Mitra, “Collision-Avoidance Radar for Bicyclist and Runners,” *2010 IEEE National Aerospace and Electronics Conference*, 14-16 July 2010, Dayton, Ohio